

Check for updates

# Green Solvent Enabled Perovskite Ink for Ambient-Air-Processed Efficient Inkjet-Printed Perovskite Solar Cells

Vinayak Vitthal Satale, Sagnik Chowdhury, Asmaa Mohamed, Do-Hyung Kim, Sinyoung Cho, Jong-Soo Lee, and Jae-Wook Kang\*

Perovskite ink based on a green or non-toxic solvent meets industrial requirements for efficient perovskite solar cells (PSCs). Perovskite inks must be developed with non-toxic or involve the limited use of toxic solvents to fabricate efficient inkjet-printed (IJP) perovskite photovoltaics. Herein,  $\gamma$ -valerolactone is used as a solvent with a low environmental impact, and the strategy showed category 3 toxicity, even with a small quantity of toxic solvents employed to dissolve the perovskite salts. The structural, optical, and electronic properties of IJP perovskite films are improved by adding 1,3-dimethyl-2-imidazolidinone (DMI) to the green perovskite ink. The IJP perovskite films developed by green solvents with 15% (volume %) of DMI exhibited high thickness uniformity ( $\approx$ 97%), and thicker and smoother surfaces than their counterparts. An additive-modified IJP-PSC device achieved a maximum power conversion efficiency (PCE) of 17.78%, higher than that of an unmodified device (14.75%). The performance of the IJP-PSC device is superior primarily because of its exceptional film-thickness homogeneity, larger grains, and appropriate structures. These attributes significantly decreased unwanted reactions of the perovskite with solvents, ensuring phase purity and enhancing overall efficiency. The innovative green-solvent ink-engineering strategy for producing large-scale perovskite films shows great promise for advancing perovskite solar module technology (with PCE of 13.14%).

1. Introduction

Solution-processable perovskites are gaining attention due to their outstanding light-absorption properties and remarkable defect tolerance and are a promising competitor of silicon solar technologies.<sup>[1,2]</sup> Recently, perovskite solar cells (PSCs)

have achieved an impressive power conversion efficiency (PCE) of 26.7%.[3] The low environmental impact and sustainability associated with perovskites, along with the extended duration of growth processing for controlling perovskite grain growth are crucial to the successful commercialization of perovskite photovoltaics. Multiple alternative fabrication techniques have proven to be effective for large-scale production including slot-die, screen printing, spray printing, and inkjet-printed (IJP) PSCs.[4] Piezoelectric drop-on-demand inkjet printing delivers significant advantages, including precise control over the fabrication process, minimal waste of ink, and increased throughput.[5] High-quality, IJP, triple-cation perovskite layers comprising methylammonium, formamidinium, and cesium have been developed with thicknesses exceeding 1 µm and achieved a maximum PCE of greater than 21%.[6] Recently, Pesch et. al., employed duel strategy (thermally evaporated inorganic lead iodide and IJP organic cation precursors) to obtain the better-quality perovskite films and reached their PSC (p-i-n type) device performance

up to 18.2%.<sup>[7]</sup> Inkjet printing has allowed remarkable advances in the field of scaling up the photovoltaics; Panasonic has developed an IJP perovskite solar module with a device area of 800 cm², achieving a PCE of ≈16.09%.<sup>[8]</sup> However, challenges remain, including ink stability, nozzle clogging, and the

V. V. Satale, S. Chowdhury, A. Mohamed, J.-W. Kang Department of Flexible and Printable Electronics LANL-CBNU Engineering Institute-Korea Jeonbuk National University Jeonju 54896, Republic of Korea E-mail: jwkang@jbnu.ac.kr

The ORCID identification number(s) for the author(s) of this article can be found under https://doi.org/10.1002/adfm.202503717

© 2025 The Author(s). Advanced Functional Materials Published by WILEY-VCH GmbH. This is an open access article under the terms of the Creative Commons Attribution License, which permits use, distribution and reproduction in any medium, provided the original work is properly cited.

DOI: 10.1002/adfm.202503717

A. Mohamed
Department of Physics
Faculty of Science
South Valley University
Qena 83523, Egypt
D.-H. Kim
KEPCO Research Institute

Korea Electric Power Corporation 105 Munji-Ro, Yusung-Gu, Daejeon 34056, Republic of Korea S. Cho, J.-S. Lee

Department of Energy Science and Engineering Daegu Gyeongbuk Institute of Science and Technology (DGIST) Daegu 42988, Republic of Korea www.advancedsciencenews.com



www.afm-journal.de

coffee-ring effect. Case studies must systematically address these issues to provide justifiable solutions to inkjet printing. [9-11] To attain superior-quality perovskite films and demonstrate high efficiency in the industrial production of PSCs, several essential measures, such as usage of non-toxic solvents and additive engineering in perovskite inks must be implemented.

A solvent mixture containing  $\gamma$ -valerolactone (GVL), a nontoxic compound derived from biomass, has drawn considerable research interest. GVL can be extracted efficiently through the hydrogenation of levulinic acid, a byproduct of the hydrolysis of lignocellulose. While it is predominantly used as a food additive, GVL has shown considerable promise in the separation and conversion of biomass.[12] GVL also has low toxicity (a median lethal dose;  $LD_{50} = 8800.0 \text{ mg k}^{-1}\text{g}$ ), a high boiling point (207.0 °C), a high flash point (96.1 °C), and a low freezing point  $(-31.0\,^{\circ}\text{C})$ . [13–15] Compared with green solvents such as isopropyl alcohol, ethanol, DMSO, and triethyl phosphate, the GVL reportedly enhance chemical bonding with FA+ to increase their stability in perovskite inks and helps to form a uniform film.[12,16] Additionally, [PbIx]<sup>2-x</sup> complexes can promote the formation of superior photoactive perovskite films with better morphology.[17,18] Given the advantages of GVL, Worsley et al. aimed to develop a green precursor ink for IJP perovskite photovoltaic (PV) devices and achieved PCEs of 12.9% and 13.82%.[16,19] Chalias et al. modified a perovskite ink with GVL with a reduced solution concentration.[20] Their carbon-based, hole-transport-materialfree device, an IJP PSC, achieved PCEs of 13.07% for small areas and 8% for modules. However, the performance of IJP perovskite systems remains inadequate for industrial applications, even after introducing a green solvent. Future modifications to such types ink are essential to improve the quality of the perovskite film and ensure scalability. These modifications should involve greener solvents with minimal or limited amounts of dimethylformamide (DMF) and dimethyl sulfoxide (DMSO), as well as the inclusion of solvent additives with a high boiling point[9,21].

To promote environmentally friendly perovskite processing using inkjet printing, we developed a green perovskite ink with a non-toxic solvent and additon of 1,3-dimethyl-2imidazolidinone (DMI) as an additive. We explored the effects of this ink on film properties and assessed the performance of PV devices. The greener nature and exceptional chemical properties of the ink suppressed nozzleclogging and the coffee-ring effect and formed uniform perovskite films over the substrate. The green solvent with additive engineering enabled the formation of thicker, smoother, and highly uniform films in which larger grains of a purer perovskite phase were embedded, improving the optoelectronic properties of IJP perovskite. The enhanced grain size of the IJP perovskite films decreased the number of defects dramatically and controlled charge recombination. Additionally, the green solvent with additives improved the surface texture, resulting in superior uniformity and improved optical and electronic properties. IJP PSCs fabricated with an environmentally friendly solvent containing a minimal amount of a high-boiling-point solvent as an additive achieved an efficiency of 17.78% and demonstrated exceptional durability.

Adv. Funct. Mater. 2025, 35, 2503717

#### 2. Results and Discussion

#### 2.1. Inkjet-printed Perovskite film fabrication

Green solvent-based IJP PSCs were developed in an n-i-p type structure using the process described in sub-point 1 of the Supplementary Information (SI) with a green solvent-based IIP perovskite as the primary absorber layer. Solvent characteristics are determined primarily by their Hansen parameters, such as  $\delta_{\mathrm{D}}$ (dispersive),  $\delta_{\rm P}$  (polar), and  $\delta_{\rm H}$  (H-bonding), which are summarized in Table S2 (Supporting Information). Generally, solvents with high  $\delta_D$  are considered to be toxic solvents as compared to the solvents with low  $\delta_{\rm D}$ . GVL, which reportedly has a lower  $\delta_{\rm D}$  (16.7 MPa<sup>1/2</sup>), compared with N-methyl-2-pyrrolidone (NMP), DMF, and  $\gamma$ -butyrolactone (GBL), identified as a greener solvent. Considering these benefits of GVL, Kim et al. employed GVL with DMSO to accelerate the perovskite precursor properties and developed eco-friendly spin-coated PSC devices with a PCE of 20%.[22] Similarly, to accelerate the chemical reaction between the perovskite and ternary solvent system, we chose GVL with minimal amounts of DMF, DMSO, and DMI (Table \$1, Supporting Information). Here, we investigated GVL as a green solvent with DMI additive at 10%, 15%, and 20% concentrations to evaluate IJP perovskite film properties and device performance. Due to DMI's high boiling point, over 20% remain in the matrix, significantly altering growth and optoelectronic properties.[21] Smaller amounts (above 10%) have a minimal effect on perovskite ink and film properties. To understand DMI's impact on our green solvent system-based perovskite ink, we focused on 10-20% concentrations. The toxicity of individual solvents and their effects on humans, animals, and the environment have been investigated. The toxicity level of mixed solvents needs to be explored to understand their potential for industrialization. To determine the mixed solvent's toxicity, the acute toxicity estimation (ATE) formula was used (Expression S1, Supporting Information) as illustrated in Figure S1 (Supporting Information). The estimated dermal  $(ATE)_{mix}$  for the green solvent (GVL:DMF:DMSO) at a ratio of 46:28:26 (v%) was 3191.6 mg  $k^{-1}\text{g}\text{,}$  and the dermal (ATE)  $_{\rm mix}$  for green+DMI-20 (GVL:DMI:DMF:DMSO) at a ratio of 26:20:28:26 (v%) was 2560.2 mg k<sup>-1</sup>g. World Health Organization acute hazard rankings for dermal ATEs are provided in Table S4 (Supporting Information). The range of (ATE)<sub>mix</sub> values (Figure S1, Supporting Information) for the green solvent and the green solvent with DMI was 2000-5000 mg  $k^{-1}$ g (category 3). These values indicate that our mixed solvent system yields only slightly or minimally toxic and not harmful to animals, plants, or the environment. We explored the green solvent system to develop a perovskite layer using an inkjet printer and a process elaborated in Experimental details (S1.3,S1.4, Supporting Information). A schematic of the inkjet printing process is provided in Figure 1a and described in our earlier published works.[9,23] In the present research, the drop spacing of 15 µm and voltage of 29 V was used to obtain uniform dropping and jetting.

As shown in Figure 1b, the green solvent was modified with a DMI additive to alter the chemical properties of the perovskite ink. DMI is a non-protic polar solvent characterized by low volatility. DMI additives in perovskite precursors enhance the dissolution of perovskite salts in greener solvent systems (here, GVL with minimal DMF and DMSO). This leads to a more uniform

16163028, 2025. 40, Downloaded from https://advanced.onlinelibrary.wiley.com/doi/10.1002/adfm.202503717 by Daegu Gyeongbuk Institute Oft, Wiley Online Library on [03/12/2025]. See the Terms and Conditions (https://onlinelibrary.wiley.com/terms-

and-conditions) on Wiley Online Library for rules of use; OA articles are governed by the applicable Creative Common

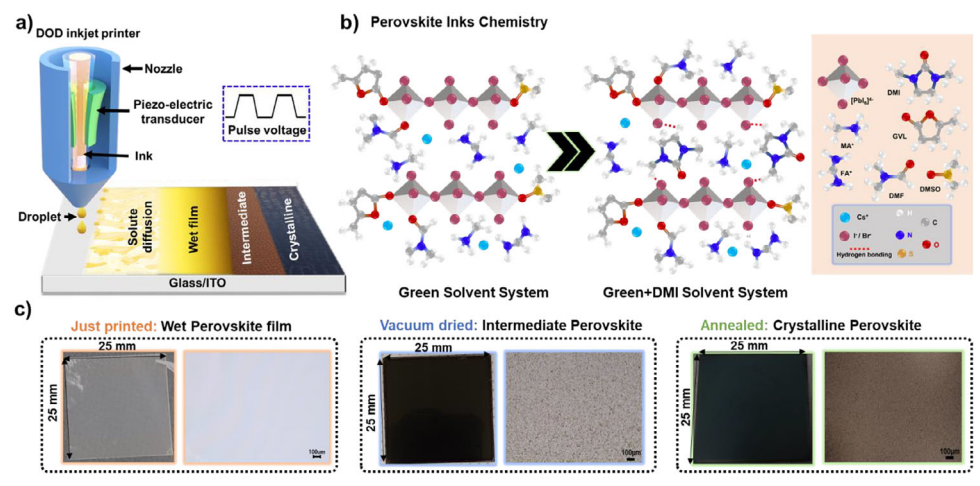


Figure 1. a) Schematic of the perovskite inkjet-printing process. b) Green perovskite ink and schematic of the perovskite ink chemistry. c) Inkjet-printed perovskite film-fabrication steps (digital pictures with optical images): wet film, intermediate phase, and crystalline perovskite film.

and homogeneous distribution of perovskite complexes, improving ink homogeneity. When added to the precursor solution, DMI interacts with metal halide ions and organic cations, influencing the nucleation and crystallization processes during film formation. DMI with an azole and a C=O group that effectively donates a lone electron pair from the oxygen atom of the C=O (Figure 1b). This interaction forms a Lewis adduct with PbI<sub>2</sub>, which controls the perovskite's grain growth. [9,21] As it is less carcinogenic than hexamethylphosphoramide and poses relatively less reproductive toxicity, NMP facilitates the DMI approach because it provides a safer working environment.[21,24,25] Here, DMI (10%, 15%, and 20% by volume) was incorporated as an additive solvent into the GVL:DMF:DMSO to accelerate the properties of the perovskite ink and improve the quality of the IJP perovskite films. The dipole moment of GVL and DMI (≈4.3 D) is higher than those of DMF (3.86 D) and DMSO (3.96 D), providing a more stable intermediate phase of triple cationic perovskite. [26] This strategy produced a uniform IJP perovskite wet film, as illustrated in Figure 1c by digital and optical images of IJP perovskite films. Film fabrication was completed by vacuum drying, which evaporated the solvent and obtained a highly crystalline phase via annealing at 150 °C under ambient conditions. An antisolvent-free solvent evaporation technique, i.e., vacuum evaporation of solvents at 5  $\times$  10<sup>-3</sup> Torr for several minutes. Afterward, perovskite films were transferred immediately to a hot plate for the annealing process at 150 °C for 20 min. These two steps help to evaporate the solvents completely, even with a small amount of DMI (15%). The postannealing temperature was plugged at 150 °C to avoid the thermal decomposition of the perovskite film. An excessively high annealing temperature (>150 °C) will trigger the migration of halide ions from the perovskite lattice and lead to the phase transformation of  $\alpha$ -FAPbI<sub>3</sub> perovskite into the PbI<sub>2</sub> phase. [9,27,28]

#### 2.2. IJP-Perovskite film nucleation and crystallization

Incorporating the non-volatile additive DMI in the perovskite ink substantially prolongs the growth duration of perovskites, ensuring the creation of top-notch perovskite films. To investigate the role of DMI additive (at 0%, 10%, 15%, and 20%; v%) in the nucleation and crystallization kinetics of the perovskite precursor inks (green solvent-based), the natural drying process of the IJP films with green and green+DMI-15 solvents was compared. As revealed by an optical microscope, as shown in Figure 2a, IJP films with the green solvent initially (after 10 min) formed relatively small nuclei within the film through a random Poisson process.<sup>[29]</sup> These nuclei then underwent rapid 1D growth, producing dendrites up to several hundred um in length.[30,31,26] In contrast, with the green+DMI-15 ink, growth took 30 min, confirming that adding the DMI additive significantly affected the nucleation and perovskite growth processes. We found dramatically decreased growth rates of dendrites under natural drying, and many small grains were visible, enabling the formation of larger grains after drying and annealing.[9,26] The viscosity and surface energy (at 23 °C) of the solvents are outlined in Table \$5 (Supporting Information). The viscosity of the green ink, recorded at a room temperature of 23 °C, was 3.7 cPs. However, it increased to 4.0 cPs after introducing DMI (15%) additives. The surface energy of the ink formulated with the green solvent and DMI-15 was 39.2 N m<sup>-1</sup>, which exceeded that of the green solvent-based perovskite ink (38.4 N m<sup>-1</sup>). The higher surface energy observed for the green+DMI-15 perovskite ink suggests that it could control the spreading rate.<sup>[9]</sup> The precise distribution of perovskite ink with an environmentally friendly solvent and DMI eliminated ink spillage throughout the printing process, ensuring a uniform film. Additionally, the moderately viscous perovskite ink played a crucial role in managing the flow across the printed substrate, resulting in a consistently high-quality perovskite film. Compared with the green ink, the green+DMI-15 ink greatly enhanced the ink property and altered the perovskite film quality. The DMI (higher boiling point than counterparts) additive, which has the ability to control capillary flow, ensured a perovskite film with superior uniformity and morphology. The green+DMI-15 ink had a thickness uniformity of  $\approx$ 97%, greater than the 95% observed for the green ink. The thickness uniformity study is included in a 3D profile plot in Figure 2b. The IJP perovskite films formulated with a green solvent demonstrated an average thickness of 437 ± 8 nm and

1616289.2025, 40, Dwnholoded from https://dwnneed.onlinelibrary.wiky.com/d/010.002/adfn20.2059171 by Daegu Gyongbkt Institute Of, Wiley Online Library on [03/12/2025]. See the Terms and Conditions (https://onlinelibrary.wiky.com/terms-and-conditions) on Wiley Online Library for rules of use; OA articles are governed by the applicable Cerative Commons

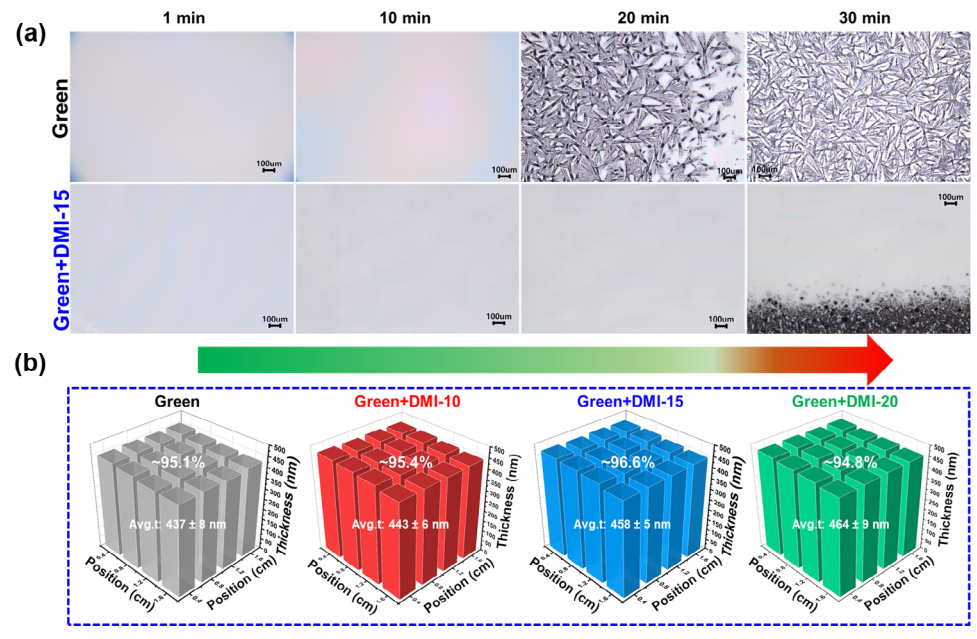


Figure 2. a) Optical microscope images of the natural drying and crystallization of green and green+DMI-15 solvent-based IIP perovskite precursor films. b) A thickness uniformity study of green and DMI additive-engineered solvent-based IJP perovskite films (25 mm × 25 mm) measured using an alpha step.

thickness uniformity of 95.1%. In contrast, the films produced using a green+DMI-15 solvent achieved an average thickness of  $458 \pm 5$  nm, with thickness uniformities reaching 96.6%. This improvement is evidence of the effectiveness of the DMI additive in controlling capillary and Marangoni flow during printing.[9] Indeed, we observed improved film uniformity with the DMI additive; the negligible or minor coffee-ring effect was seen after the solvent drying and annealing process. This phenomenon was attributed to solvent evaporation and crystal growth due to solution flow, solute diffusion, solvent drying, and crystal growth. However, these negligible effects do not affect the film quality and their optoelectronic properties significantly.[32,33] Inkjet printing precisely deposits minimal amounts of ink over different types of substrates, which has advantages over spin-coating in industrial applications.[34] The perovskite films produced through inkjet printing with the green+DMI-15 solvent exhibited excellent uniformity and increased thickness and are suitable for largearea device applications. Additionally, Fourier transform infrared spectroscopy (FTIR) analysis of the solvents and their mixture (Figure S2a, Supporting Information) was used to investigate the chemistry of the ink and the mechanism responsible for perovskite growth. A major peak (Figure S2a, Supporting Information) at 1680-1660 cm<sup>-1</sup> in the spectra for the DMI solvent and DMI-additive-engineered inks corresponds with C=N stretching vibrations and suggests strong interactions between the solvent and FA+/MA+ complexes. [9,35,36] The addition of DMI to the green ink could strengthen the bonds between the solvent and FA+/MA+ complexes, slowing the inkdrop spreading rate and perovskite grain growth, as can be seen in Figure 2a and promoting the production of more uniform films. Furthermore, a shift of 1-2 cm<sup>-1</sup> in the peak to lower energies by incorporating additives in the perovskite ink could influence the structure of the perovskite and the hybridiza-

tion state, potentially helping create a purer phase with fewer defects [35-37].

## 2.3. Optical, structural, and morphological study of IJP-Perovskite film

The IJP perovskite films made using the green solvent and DMIadditive inks demonstrated an absorption edge near 770 nm, as shown in Figure 3a. The inclusion of DMI in the solvent resulted in increased absorption. Analysis of the optical bandgap  $(E_a)$  values, derived from the Tauc plot seen in the inset of Figure 3a, revealed a decrease in  $E_{\sigma}$  from 1.65 to 1.62 eV with the incorporation of DMI (15%) into the green solvent. The addition of DMI into the green solvent system tuned the optical properties of the perovskite films by influencing their absorbance and band gap values. A well-formed perovskite film with larger gains typically exhibits better optical properties, improving light absorption and photon-to-electron conversion efficiency in solar cells.<sup>[9]</sup> Furthermore, the structural characteristics of the IJP perovskite films produced with green and DMI additive-engineered inks were examined using X-ray diffraction. The spectral analysis depicted in Figure 3b for IJP perovskite films produced using a green solvent and a green solvent with DMI additives revealed a significant peak associated with the (001) plane at a  $2\theta$ diffraction angle of 14.2°. In addition to this primary peak, several other notable peaks corresponding to the (011), (111), (002), (012), (112), (022), and (003) lattice planes were evident, confirming the cubic crystallographic phase of the perovskites. [9,23] The intensity of the peaks for the green+DMI-15 ink was markedly higher than that of the standard green ink, suggesting an enhancement in crystallinity. The crystallite sizes, seen in Figure 3c, were estimated using the equation  $D = k\lambda/\beta Cos\theta$ , where *D* is the



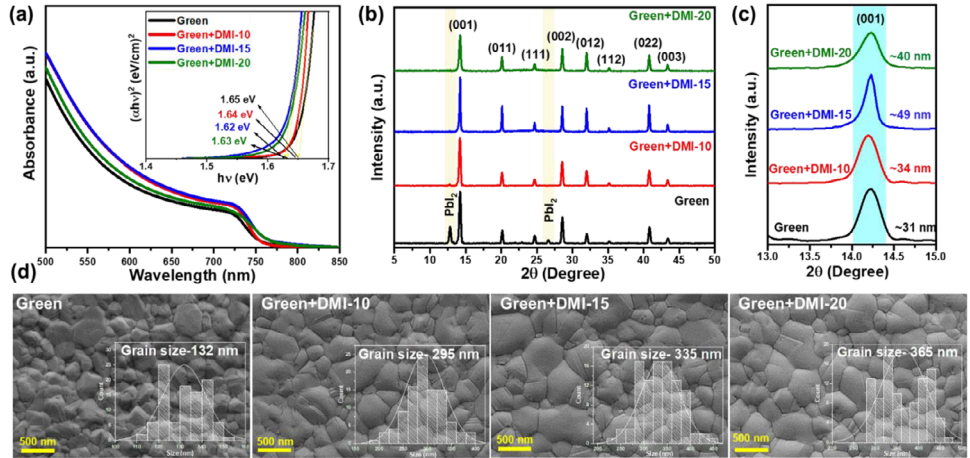


Figure 3. a) Ultraviolet-visible spectra and a Tauc plot (inset), b) X-ray diffraction patterns, and c) extrapolated perovskite prominent (001) peak of the green- and green+DMI solvent-based IJP perovskite films. d) Surface morphologies with grain-size distributions (inset) of green- and green+DMI solvent-based IJP perovskite films.

crystalline size of perovskite, k is the Scherrer constant (0.98),  $\lambda$  is the wavelength (1.54 Å), and  $\beta$  is the full width at half maximum. The crystalline size was  $\approx 31$  nm for the green film, increasing to 49 nm for the green+DMI-15 film. [9] These findings highlight the influence of additive engineering on the structural characteristics of IJP perovskite films. An IJP perovskite film made with a green solvent (without DMI additive) showed a smaller intensity peak at  $2\theta=12.7^{\circ}$  (PbI<sub>2</sub>). The weak interaction of GVL to PbI<sub>2</sub> can produce the PbI<sub>2</sub>-secondary phases in the film, which compromises the quality of Perovskites. [922] However, adding DMI altered the chemical reactions between the solvents and perovskite complexes; the PbI<sub>2</sub> peak decreased, and a pure cubic-phase perovskite film was obtained. The strong interaction of DMI with PbI<sub>2</sub> helps to dissolve perovskite complexes thoroughly and form purer phase perovskites. [9,25]

The surface elemental compositions of the IJP perovskite films prepared with green and DMI additive-engineered solvents are shown in Figure S4a-f (Supporting Information). The analysis identified six key elements in both IJP films. The XPS spectra for all elements were fitted individually; the peak intensity of these elements was higher in the case of the green+DMI-15 solvent compared with that of the green solvent, similar to an effect reported previously.[37-39] The effect of the DMI additive on perovskite grains was studied systematically by a fieldemission scanning electron microscope (FE-SEM). The IJP perovskite film micrographs in Figure 3d indicate that DMI additive (15%) films exhibit significant uniformity, compactness, and pinhole-free surface compared to the green solvent processed film, as illustrated in the accompanying histogram (inset). The grains in the films produced with a DMI additive were larger than those fabricated with the green solvent alone.<sup>[21]</sup> The estimated grain sizes of the IJP perovskite film produced with the green+DMI-15 solvent were ≈335 nm in size, in contrast to the 132 nm grains observed for the films with only the green solvent. The combination of DMI and GVL produced a synergistic effect that prolonged the crystallization process and effectively influenced the gain size. Similar effects have been observed in previous works that explore the DMI additive (which has a boiling

point of  $\approx$  225 °C), which allowed slower grain growth in the perovskite, forming larger grains.<sup>[9,21]</sup>

#### 2.4. Electronic properties and roughness of IJP-Perovskite film

The electronic characteristics of IJP perovskite films were investigated through ultraviolet photoelectron spectroscopy (UPS), as illustrated in Figure 4a. To derive the band parameters, we applied the methods listed in (Expression S2-S4, Supporting Information). The compiled findings presented in Table S7 (Supporting Information) indicate that the film based on the green+DMI-15 solvent exhibited a comparatively smaller conduction band offset and a larger valence band offset compared with the standard green-solvent film. The enhanced charge-collection efficiency at the interface between the electron transport layer (ETL) and the perovskite layer is depicted in Figure 4b. The addition of DMI altered the electronic properties of the perovskite films, possibly due to the formation of the highly pure phase of perovskite and larger grains than the green one. These findings point to enhanced performance of perovskite-based devices, as optimized charge-transport mechanisms are essential for improving efficiency in photovoltaic applications.<sup>[9]</sup> By carefully analyzing UPS data and associated band-structure parameters, we can obtain deeper insights into the electronic behavior that governs the interactions between these layers, ultimately contributing to more effective charge separation and collection in solar cells.

The charge-transfer dynamics of the IJP perovskite samples were examined using time-resolved photoluminescence (TRPL) spectra, as depicted in Figure 4c. The findings indicate that the green+DMI-15 sample exhibited noticeably slower photoluminescence (PL) decay compared with the other samples, including the standard green, green+DMI-10, and green+DMI-20 configurations. This observation confirms that the strategic incorporation of specific additives can effectively mitigate trap states within the bulk material, enhancing the perovskite films' overall quality. The PL decay lifetime ( $\tau_{\rm PL}$ ) was calculated by fitting a quadruple-exponential decay function (Expression S5,

1616280.2025, 40, Dwnholoded from https://dwnneed.onlinelibrary.wiky.com/ob/10.1002/adfin20.203717 by Daegu Gyeongbuk Institute Of, Wiley Online Library on [03/12/2025]. See the Terms and Conditions (https://onlinelibrary.wiky.com/terms-and-conditions) on Wiley Online Library for rules of use; OA attacks are governed by the applicable Centwie Commons

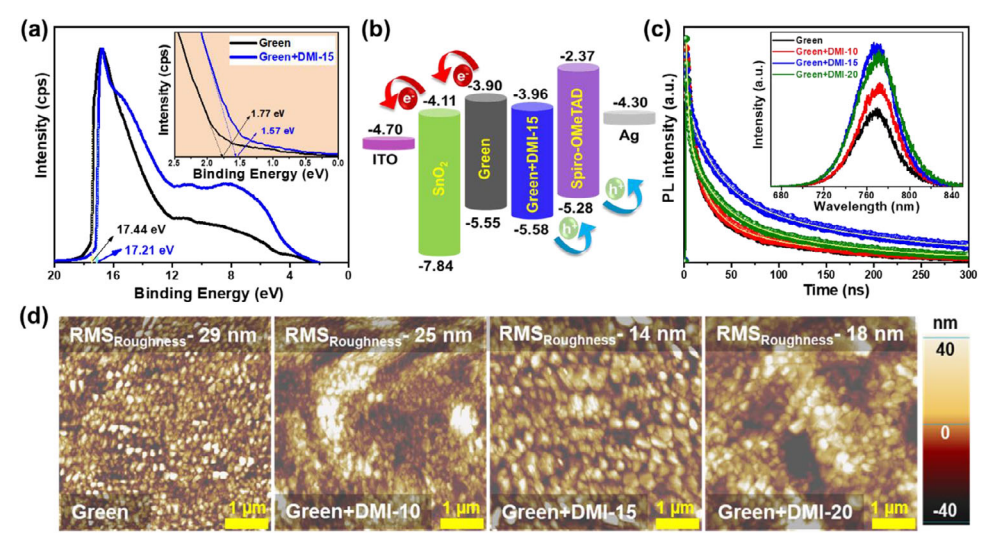


Figure 4. a) The cut-off and magnified-onset regions (inset) of ultraviolet photoelectron spectroscopy spectra. b) Schematic of energy-level IJP PSC devices developed using a green solvent with DMI-additive engineered inks. c) Time-resolved photoluminescence and steady state photoluminescence (inset) spectra. d) Atomic force micrographs of IJP perovskite films developed using green solvents with DMI-additive—engineered inks.

Supporting Information) using the respective values for  $\tau_1$ ,  $\tau_2$ ,  $\tau_3$ , and  $\tau_4$  in Table S8 (Supporting Information). [40] A PL mapping study further confirmed the uniformity of the electronic properties across the film surfaces, as illustrated in the decay images in Figure S5 (Supporting Information). The average  $\tau_{\rm PL}$  for the IJP perovskite film increased significantly from ≈109 ns for the reference green sample to ≈229 ns for the green+DMI-15 sample. This degree of enhancement underscores the pivotal role of additive engineering in suppressing trap levels, which directly reduce non-radiative carrier-recombination centers within the bulk material. However, adding DMI (20%) showed decreased PL intensity and faster PL decay than the DMI-15. This may be due to the thicker film formation with excess DMI. As seen in Figure 3c, the (001) diffraction peak gradually shifted from  $\approx 14.23^{\circ}$  to  $\approx 14.22^{\circ}$ as the film thickness increased by adding DMI (15% to 20%). The peak shift to a lower diffraction angle indicated an expansion of the perovskite lattice with increasing film thickness (excess DMI). This could be attributed to the strain effect induced by the excessive DMI, which may develop unintended defects in bulk.[41] In Figure 4c, the green+DMI-15 sample has a distinct PL emission peak at 771 nm. In contrast, the green, green+DMI-10, and green+DMI-20 samples have emission peaks at 768, 769, and 770 nm, respectively. The reduction of recombination centers in the IJP perovskite samples, achieved through additive engineering, indicates significant improvements in both the quality and efficiency of the produced perovskite films. This paves the way for high-performance perovskite materials that are wellsuited to a range of optoelectronic applications. The atomic force micrographs in Figure 4d reveal a strong correlation with the results from the FE-SEM analysis. The root mean square roughness values were ≈29 nm for the pure-green sample, 25 nm for the green+DMI-10, 15 nm for the green+DMI-15 sample, and  $\approx$ 20 nm for the green+DMI-20 sample. The green+DMI-15 sample displayed exceptional uniformity and smoothness and is an ideal candidate for scalable device fabrication and module processing. Such smoothness and uniformity are expected to enhance performance and reliability in practical applications, indicating these films as a compelling choice for future developments in the field.

## 2.5. IJP-Perovskite solar cell device performance

We undertook a comprehensive investigation of the performance of n-i-p type IJP PSC devices that use green- and green+DMI solvent-based perovskite inks. The fabrication process for these devices is depicted in supporting information (sub-point 1.4) and a schematic IJP PSC device is illustrated in Figure 5a. We attempted to shed light on the effects of environmentally friendly solvents on solar cell efficiency and overall effectiveness, highlighting the significance of sustainable energy solutions in contemporary technology. The cross-sectional image in Figure 5b confirms the successful formation of all functional layers within the green+DMI-15 IJP-PSC device. This illustrates the proper stacking and arrangement of these layers and highlights the impressive development of larger perovskite grains. This is robust evidence of the successful development and distinct advantages of an innovative perovskite solar cell design. The device parameters were systematically derived from the current-voltage (I-V)characteristics analysis, as depicted in Figure 5c. Our investigation focused on the effect of additive-engineered perovskite inks on device performance. The resulting parameters are thoroughly outlined in Table 1.

We observed that PSCs developed with green+DMI-15 ink achieved a PCE of 17.78%, significantly exceeding that of the devices that used green ink alone (14.57%). Additionally, PSCs produced using green+DMI additives at varying concentrations (green+DMI-10 and green+DMI-20) demonstrated relatively high efficiencies of ≈16.45% and 15.99%, respectively. Control experiments were conducted using spin-coated PSCs with the same green and green+DMI-15 inks to validate these results. The comparative results in Figure S6a (Supporting Information)

16163028, 2025, 40, Downloaded from https://advanced.onlinelibrary.wiley.com/doi/10.1002/adfm.202503717 by Daegu Gyeongbuk Institute Of, Wiley Online Library on [03/12/2025]. See the Terms and Conditions (https://onlinelibrary.wiley.com/terms-

and-conditions) on Wiley Online Library for rules of use; OA articles are governed by the applicable Creative Commons

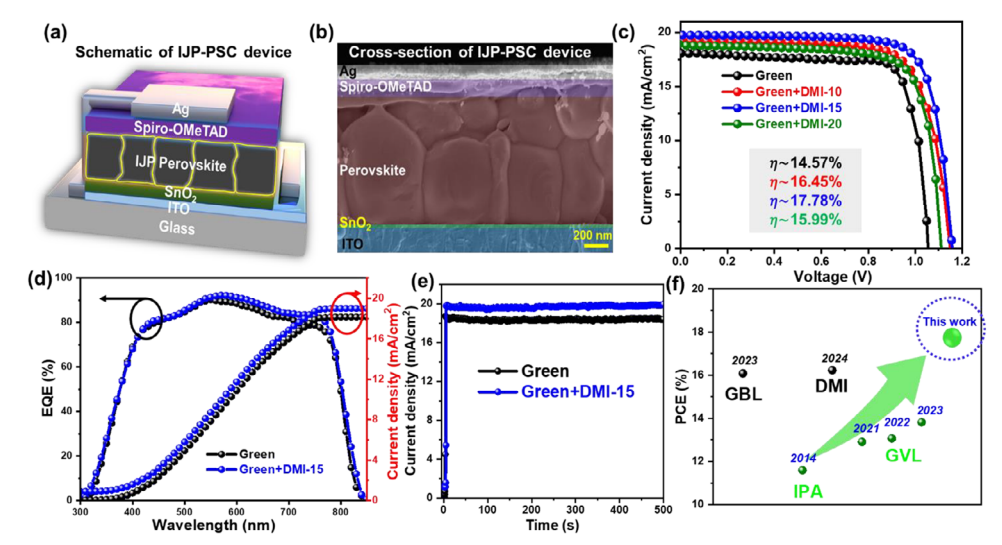


Figure 5. a) A schematic representation and b) a cross-sectional FE-SEM image of a green solvent-based I/P-PSC device. c) Current-voltage characteristic, d) external quantum efficiency spectra along with integrated  $J_{SC}$ , and e) steady-state  $J_{SC}$  (at the maximum power) of the green solvent and DMI additiveengineered IJP perovskite device. f) PCEs value of green-solvent IJP PSCs devices compared with previous reports.

illustrate the performance differences among the various formulations. Spin-coated PSC devices with the green solvent (PCE-15.71%) showed lower PCEs than the green+DMI-15 devices (PCE- 18.22%). Green solvent-based precursor ink is effectively used in well-known methods such as spin coating.[12] Compared to existing technologies, PSCs excel in energy efficiency, material usage, and cost, but scaling issues persist. Re-evaluating costly materials and energy-intensive methods could improve their environmental impact. Inkjet printing is a promising non-contact method suitable for different materials, patterns, and substrates, making it ideal for large-scale applications. Its low cost and use of nontoxic solvents provide significant advantages for scalable development in the solar industry.<sup>[42]</sup> This analysis establishes the effectiveness of the green+DMI-15 formulation in enhancing the efficiency of solar cells. The IJP PSC devices produced using a blend of green and DMI-15 solvents matched the performance of spin-coated counterparts, achieving a high PCE. The hysteresis study (Figure S6b, Supporting Information) of green+DMI-15 with low HI value indicates a better quality of device formation. Larger grains (as seen in Figure 3d) strongly correlate with improved charge-transport properties (Figure 4a) and enhance overall device performance. Also, it can be attributed to superior film uniformity, increased crystallinity, and high absorption of light, all of which are crucial to maximizing light tracking and energy conversion. It confirms that adding DMI additives in greensolvent systems can create ideal conditions for producing devices with superior efficiency and stability, a similar effect of DMI as seen in previous studies.[9,21,33]

These devices exhibited a  $I_{SC}$  of 19.75 mA cm<sup>-2</sup>, exceeding the 18.34 mA cm<sup>-2</sup> achieved by devices produced using the green solvent without DMI. Additionally, the proposed devices show a significant improvement in  $V_{OC}$  to 1.158 V compared with 1.055 V for green-solvent-alone devices. The compactness of the film and larger grains in the green+DMI-15 devices enhanced both charge separation and transport.[9] We further investigated trap density (N<sub>t</sub>) for IJP PSC (ITO/SnO<sub>2</sub>/IJP-perovskite/PCBM/Ag) via the space charge limited current (SCLC) method (Figure S7a,b, Supporting Information). The trap-filled limited voltage  $(V_{TEI})$ was extracted from Figure S7a (Supporting Information), and  $N_t$ was estimated using Expression S7 (Supporting Information). The defect density was reduced by adding the DMI additive to the green solvent system from  $5.165 \times 10^{16}$  cm<sup>-3</sup> (green) to  $1.972 \times 10^{16} \text{ cm}^{-3}$  (DMI-15). The trap density was considerably reduced with DMI (up to 15%), confirming that DMI can increase the grain size and effectively suppress the recombination center.[33,43-45] In contrast, the trap density increased upon increasing the DMI concentration (i.e., 20%), leading to unintended defect formation, further affecting the device V<sub>OC</sub>.

The combination of a green solvent and a DMI additive can improve the performance of IJP PSCs, paving the way for more

Table 1. Photovoltaic performance of green solvents and additive-engineered IJP PSC devices.

Devices	V <sub>OC</sub> [V]	J <sub>SC</sub> [mA/cm <sup>2</sup> ]	FF [%]	PCE [%]	Avg. PCE a) [%]
Green	1.055	18.34	75.34	14.57	14.20 ± 0.7
Green+DMI-10	1.149	19.24	74.37	16.45	$15.27 \pm 0.6$
Green+DMI-15	1.158	19.75	77.76	17.78	$17.42 \pm 0.2$
Green+DMI-20	1.111	18.82	76.51	15.99	15.68 ± 0.8

 $<sup>^{</sup>m a)}$  Statistical data for the average PCE of 20 devices.

16163028, 2025, 40, Downloaded from https://advanced.onlinelibrary.wiley.com/doi/10.1002/adfm.202503717 by Daegu Gyeongbuk Institute Of, Wiley Online Library on [03/12/2025]. See the Terms and Conditions (https://onlinelibrary.wiley.com/erms

and-conditions) on Wiley Online Library for rules of use; OA articles are governed by the applicable Creative Commons

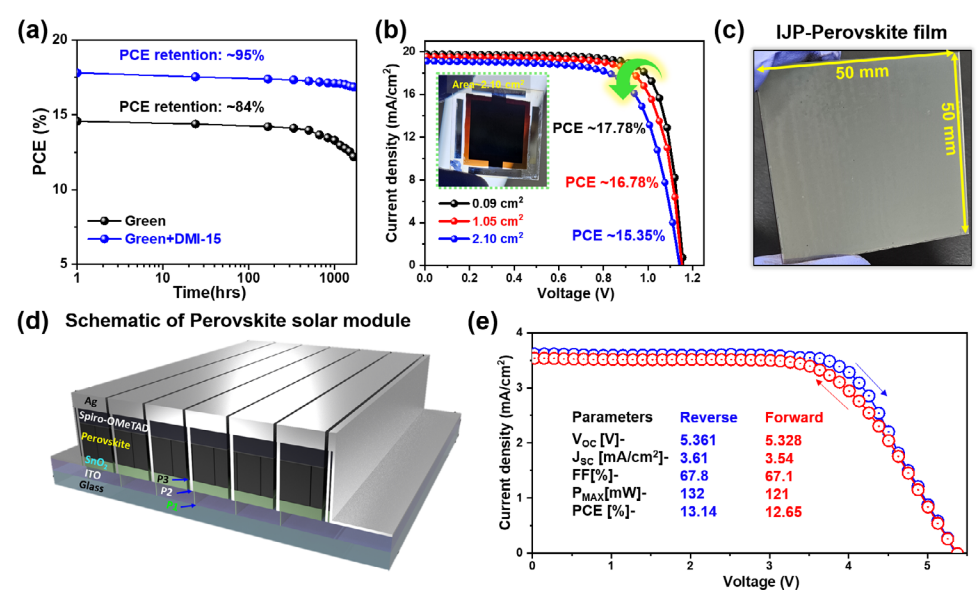


Figure 6. a) Device stability of green- and green+DMI-15 solvent-based IJP perovskite devices measured at ambient conditions. b) J-V curves of green solvent with additive modified IJP-PSCs device different active areas (inset; actual picture of 2.10 cm<sup>2</sup> active area device). c) Actual picture of 50 mm  $\times$  50 mm of the IJP-perovskite film made with additive-engineered ink. d) Schematic of IJP-perovskite solar module. e) J-V characteristic of the IJP perovskite solar module made with additive-engineered ink.

efficient and high-quality photovoltaic devices. Integrated  $J_{SC}$  values for green and additive-engineered (DMI-15) devices were obtained using external quantum efficiency (EQE) data, as shown in Figure 5d. The  $I_{SC}$  values for green (18.10 mA cm<sup>-2</sup>) and DMI-additive (19.15 mA cm<sup>-2</sup>)-engineered devices were closer to the value obtained from the *J-V* curve. No perovskite film thicknesses exceeded 600 nm, and parasitic absorption loss may have occurred at the interface between the absorber and the hole transport layer (HTL), resulting in lower EQE signals near 700 nm compared with those near 550 nm. [35,46-51] Moreover, the IJP PSC devices demonstrated enhanced light-soaking stability after being illuminated for 500 s, as shown in Figure 5e. The shelf-life of the IJP PSCs with the green+DMI-15 solvent significantly outperformed those of devices made with green solvents alone, showcasing the superior light-soaking capability of the additiveengineered device. To confirm our findings, we compared device efficiencies against those reportedly previously. The data indicate that the device efficiencies of IJP PSCs made with the green+DMI-15 solvent exceeded consistently and outperformed those of other green solvent systems, as illustrated in Figure 5f and detailed in Table \$10 (Supporting Information). These results emphasize the advantages of using a DMI additive in green solvents and provide crucial insights into the future of highperformance perovskite PV technologies, with significant implications for various applications in the field. The reproducibility of the IJP perovskite devices was validated by testing 20 individual devices, as illustrated in Figure S8a,b,c,d, Supporting Information). The devices manufactured with the green+DMI-15 solvent achieved commendable performance metrics, including an average maximum  $V_{OC}$  of 1.139  $\pm$  0.01 V, a  $J_{SC}$  of 19.77  $\pm$  0.1 mA cm<sup>-2</sup>, a fill factor (FF) of 77.38  $\pm$  0.6%, and a PCE of 17.42  $\pm$  0.2%. These results fall within a remarkably narrow distribution of performance values, highlighting the high consistency and reproducibility of the device fabrication process.

In contrast, devices produced with green-only, green+DMI-10, and green+DMI-20 displayed greater variability in performance. The gree+DMI-15 has larger grains (Figure 3d) than (green and green\_DMI-10), which strongly correlates with improved charge-transport properties (Figure 4a) and enhances overall device performance. Also, green+DMI-15 is attributed to superior film uniformity, increased crystallinity, and higher light absorption than counterparts (green, green\_DMI-10, and green+DMI-20), all crucial to maximizing light tracking and energy conversion. It confirms that adding DMI additives (15%) in green-solvent systems significantly created ideal conditions for producing high-quality devices with superior efficiency and stability. Also, the superior reproducibility of the green+DMI-15 devices positions them as exceptional choices for developing scalable PSCs.

#### 2.6. Stability and scalability of IJP PSCs

Figure 6a demonstrates the long-term stability of two IJP PSCs: those using green solvents and those engineered with additives. The devices were stored under ambient conditions for 2.5 months (>1600 h) to assess the effects of aging on performance. The results revealed a notable contrast between the two formulations, with the solar cells of standard green solvents achieving a PCE retention of 84%, while devices with green solvents and an additive (DMI-15) displayed a relatively high PCE retention of 95%. The superior retention rates of PCE underscore the superior durability of these green+DMI-15 devices due to the better quality of IJP films (purer crystallinity, smoother, and uniform surface). The water contact angle increased from  $\theta = 47$  ° to  $\theta = 55$  ° by incorporation of DMI into the green solvent system (Figure S9, Supporting Information). Our previous work shows that the additive DMI can produce larger grains with smother films, forming hydrophobic surfaces that repel water. These findings

1616280.2025, 40, Dwnholoded from https://dwnneed.onlinelibrary.wiky.com/ob/10.1002/adfin20.203717 by Daegu Gyeongbuk Institute Of, Wiley Online Library on [03/12/2025]. See the Terms and Conditions (https://onlinelibrary.wiky.com/terms-and-conditions) on Wiley Online Library for rules of use; OA attacks are governed by the applicable Centwie Commons

**Table 2.** Photovoltaic performance of IJP PSC devices with different active areas and modules.

Devices active area [cm <sup>2</sup> ]	V <sub>OC</sub> [V]	J <sub>SC</sub> [mA/cm <sup>2</sup> ]	FF [%]	PCE [%]	
0.089		1.158	19.75	77.76	17.78
1.05		1.152	19.52	74.62	16.78
2.10		1.142	19.09	70.34	15.35
$\approx$ 13 (Module)	Reverse	5.361	3.61	67.88	13.14
	Forward	5.328	3.54	67.07	12.65

indicate that DMI additive engineering significantly enhances IJP-PSC devices' water and moisture stability, positioning them as potential candidates for scalable applications in real-world energy solutions. [9,33] To study the scalability of green+DMI-15 solvents-based IJP-PSC devices, we have fabricated the devices with different active areas such as 0.089, 1.05, and 2.10 cm². The J-V measurements of IJP-PSC devices with different active areas are shown in Figure 6b, and detailed J-V parameters are listed in Table 2. The scale-up process for green+DMI-15 exhibited a higher PCE retention ( $\approx$ 86%) with increased active area from 0.089 to 2.10 cm². The performances of large-area IJP PSCs were also highly consistent and reproducible.

Further, we fabricated an IJP large-scale perovskite film over a  $50 \text{ mm} \times 50 \text{ mm}$  substrate using green+DMI-15 perovskite ink, as shown in Figure 6c. Thickness was measured using the alpha step to study thickness uniformity over the IJP perovskite film, and the estimated average thickness uniformity was 92%, as depicted in Figure S10a,b, Supporting Information). The IJP perovskite solar module was fabricated to cover 50 mm  $\times$  50 mm indium tin oxide substrates with additive-engineered ink; details of the process are provided in suplimentary information, subpoint-1.4. A schematic of an IJP perovskite module is depicted in Figure 6d, and the actual picture under light is shown in Figure S10c (Supporting Information). The module comprises six cells connected in series, and the fabrication recipe follows that of our previous works.<sup>[9]</sup> In the present research, we used a condition that has been applied to small-scale devices and obtained the *J*–V curve depicted in Figure 6e. The module displayed a maximum PCE of  $\approx$ 13.14% with a  $V_{OC}$  of 5.361 V, a  $J_{SC}$  of 3.61 mA cm<sup>-2</sup>, and an FF of 67.88% (Table 2). The results support the importance of our contributions to enhancing PSC technology through printing techniques. This method offers the potential for low-cost, sustainable, and scalable production. Inkjet printing enables precise material deposition while minimizing waste, making it an effective manufacturing approach. Furthermore, the scalability of the technique is crucial for moving PSC from laboratory settings to commercial applications, addressing the growing demand for efficient solar energy alternatives.

## 3. Conclusion

This study describes a successful perovskite ink-engineering strategy using green solvents and minimal use of toxic solvents for efficient IJP PSCs. This innovative approach was demonstrated in an ambient atmosphere by combining DMI into the green-solvent system as an additive for the first time. By incorporating DMI, we successfully reduced ink toxicity while extending

the growth processing time of the films. This enhances safety and paves the way for environmentally friendly and smoother perovskite films that offer superior qualities without the need for harmful anti-solvents. The unique properties of the green solvent and additive prevent coordination with perovskite inks, resulting in compact, crystalline, and uniform structures that minimize the coffee-ring effect. Our additive-engineering strategy produces larger grains and smoother IJP perovskite films. IJP PSCs processed with this green solvent and a DMI additive achieved higher PCEs comparable to those associated with traditional green-solvent-based perovskite inks. The highestperforming DMI additive-engineered IJP PSC device achieved a maximum PCE of 17.78%. These findings represent a crucial advance in the development of green, low-cost, and scalable IJP PSCs that can be applied to industrialization and sustainable energy solutions.

## **Supporting Information**

Supporting Information is available from the Wiley Online Library or from the author.

# Acknowledgements

This work was supported by the Basic Science Research Program (NRF-2021R1A2C2004206 and NRF-RS-2023-00247038) through the National Research Foundation (NRF) of Korea, funded by the MSIT. This work was supported by the Korea Electric Power Corporation (CX72220014) and by the selection of a research-oriented professor of Jeonbuk National University in 2025. The basic characterizations were performed in the Center for University-Wide Research Facilities (CURF) at Jeonbuk National University.

## **Conflict of Interest**

The authors declare no conflict of interest.

#### **Author Contributions**

V.V.S. contributed to the conceptualization, visualization, methodology, formal analysis, data curation, investigation, original draft writing, and review and editing. S.C. contributed to the methodology, investigation, and formal analysis. A.M. was involved in the formal analysis. D.-H.K. contributed to the methodology and secured funding. S.C. contributed to formal analysis and data curation. J.-S.L. contributed to the methodology and data curation. J.-W.K. provided supervision, secured funding, and contributed to the review and editing of the manuscript.

## **Data Availability Statement**

The data that support the findings of this study are available in the supplementary material of this article.

# Keywords

additive, green-solvent, homogeneity, large-area, perovskite photovoltaics

Received: February 10, 2025 Revised: April 2, 2025 Published online: April 25, 2025



www.afm-journal.de

- [1] X. Tian, S. D. Stranks, J. Huang, V. M. Fthenakis, Y. Yang, F. You, Energy Environ. Sci. 2025, 18, 194.
- [2] Z. Saki, M. M. Byranvand, N. Taghavinia, M. Kedia, M. Saliba, Energy Environ. Sci. 2021, 14, 5690.
- [3] M. A. Green, E. D. Dunlop, M. Yoshita, N. Kopidakis, K. Bothe, G. Siefer, D. Hinken, M. Rauer, J. Hohl-Ebinger, X. Hao, *Prog. Photovoltaics Res. Appl.* 2024, 32, 425.
- [4] D. Li, D. Zhang, K. S. Lim, Y. Hu, Y. Rong, A. Mei, N. G. Park, H. Han, Adv. Funct. Mater. 2021, 31, 2008621.
- [5] X. Peng, J. Yuan, S. Shen, M. Gao, A. S. R. Chesman, H. Yin, J. Cheng, Q. Zhang, D. Angmo, Adv. Funct. Mater. 2017, 27, 1703704.
- [6] H. Eggers, F. Schackmar, T. Abzieher, Q. Sun, U. Lemmer, Y. Vaynzof, B. S. Richards, G. Hernandez-Sosa, U. W. Paetzold, Adv. Energy Mater. 2020. 10. 1903184.
- [7] R. Pesch, A. Diercks, J. Petry, A. Welle, R. Pappenberger, F. Schackmar, H. Eggers, J. Sutter, U. Lemmer, U. W. Paetzold, Sol. RRL. 2024, 8, 2400165.
- [8] Panasonic Carporation, Japan's NEDO and Panasonic Achieve the World's Highest Conversion Efficiency of 16.09 % for Largest-area Perovskite Solar Cell Module, 2020, https://news.panasonic.com/ global/press/en200207-2.
- [9] V. V. Satale, H. B. Lee, B. Tyagi, M. M. Ovhal, S. Chowdhury, A. Mohamed, D.-H. Kim, J.-W. Kang, Chem. Eng. J. 2024, 493, 152541.
- [10] H. C. Nallan, J. A. Sadie, R. Kitsomboonloha, S. K. Volkman, V. Subramanian, Langmuir. 2014, 30, 13470.
- [11] D. A. Chalkias, A. Mourtzikou, G. Katsagounos, A. Karavioti, A. N. Kalarakis, E. Stathatos, Sol. RRL. 2022, 6, 2200196.
- [12] Y. Miao, M. Ren, Y. Chen, H. Wang, H. Chen, X. Liu, T. Wang, Y. Zhao, Nat. Sustain. 2023, 6, 1465.
- [13] K. S. Teoh, M. Melchiorre, F. A. Kreth, A. Bothe, L. Köps, F. Ruffo, A. Balducci, ChemSusChem. 2023, 16, 202201845.
- [14] F. Kerkel, M. Markiewicz, S. Stolte, E. Müller, W. Kunz, Green Chem. 2021. 23, 2962.
- [15] S. Dutta, I. K. M. Yu, D. C. W. Tsang, Y. H. Ng, Y. S. Ok, J. Sherwood, J. H. Clark, Chem. Eng. J. 2019, 372, 992.
- [16] C. Worsley, D. Raptis, S. M. P. Meroni, R. Patidar, A. Pockett, T. Dunlop, S. J. Potts, R. Bolton, C. M. E. Charbonneau, M. Carnie, E. Jewell, T. Watson, *Mater. Adv.* 2022, 3, 1125.
- [17] P. Ahlawat, M. I. Dar, P. Piaggi, M. Grätzel, M. Parrinello, U. Rothlisberger, Chem. Mater. 2020, 32, 529.
- [18] B. Li, Q. Dai, S. Yun, J. Tian, J. Mater. Chem. A. 2021, 9, 6732.
- [19] C. Worsley, D. Raptis, S. Meroni, A. Doolin, R. Garcia-Rodriguez, M. Davies, T. Watson, Energy Technol. 2021, 9, 2100312.
- [20] D. A. Chalkias, A. Mourtzikou, G. Katsagounos, A. N. Kalarakis, E. Stathatos, Small Methods. 2023, 7, 2300664.
- [21] L. Zhi, Y. Li, X. Cao, Y. Li, X. Cui, L. Ci, J. Wei, Nanoscale Res. Lett. 2017, 12, 632.
- [22] B. J. Kim, H. Choi, S. Park, M. B. Johansson, G. Boschloo, M. C. Kim, ACS Sustainable Chem. Eng. 2024, 12, 13371.
- [23] V. V. Satale, N. Kumar, H. B. Lee, M. M. Ovhal, S. Chowdhury, B. Tyagi, A. Mohamed, J. W. Kang, *Inorg. Chem. Front.* 2023, 10, 3558.
- [24] C.-C. Lo, P.-M. Chao, J. Chem. Ecol. 1990, 16, 3245.
- [25] L. Xie, A. N. Cho, N. G. Park, K. Kim, ACS Appl. Mater. Interfaces. 2018, 10, 9390
- [26] J. Liu, J. Cao, M. Zhang, X. Sun, T. Hou, X. Yang, L. Xiang, X. Liu, Z. Fu, Y. Huang, F. Wang, W. Zhang, X. Hao, Adv. Sci. 2024, 11, 2410266.
- [27] P. V. Kamat, M. Kuno, Acc. Chem. Res. 2021, 54, 520.
- [28] H. B. Lee, R. Sahani, V. Devaraj, N. Kumar, B. Tyagi, J. W. Oh, J. W. Kang, Adv. Mater. Interfaces. 2023, 10, 2201658.

- [29] N. K. Noel, S. N. Habisreutinger, B. Wenger, M. T. Klug, M. T. Hörantner, M. B. Johnston, R. J. Nicholas, D. T. Moore, H. J. Snaith, Energy Environ. Sci. 2017, 10, 145.
- [30] J. Li, R. Munir, Y. Fan, T. Niu, Y. Liu, Y. Zhong, Z. Yang, Y. Tian, B. Liu, J. Sun, D. M. Smilgies, S. Thoroddsen, A. Amassian, K. Zhao, S. (Frank) Liu, Joule. 2018, 2, 1313.
- [31] T. Bu, J. Li, H. Li, C. Tian, J. Su, G. Tong, L. K. Ono, C. Wang, Z. Lin, N. Chai, X. L. Zhang, J. Chang, J. Lu, J. Zhong, W. Huang, Y. Qi, Y. B. Cheng, F. Huang, Science (80-.). 2021, 372, 1327.
- [32] J. E. Kim, S. S. Kim, C. Zuo, M. Gao, D. Vak, D. Y. Kim, Adv. Funct. Mater. 2019, 29, 1809194.
- [33] X. Chang, Y. Fan, K. Zhao, J. Fang, D. Liu, M.-C. Tang, D. Barrit, D.-M. Smilgies, R. Li, J. Lu, J. Li, T. Yang, A. Amassian, Z. Ding, Y. Chen, S. (Frank) Liu, W. Huang, Research. 2021, 2021.
- [34] C. S. Pathak, G. Paramasivam, F. Mathies, K. Hirselandt, V. Schröder, O. Maus, J. Dagar, C. Klimm, E. Unger, I. Visoly-Fisher, ACS Appl. Energy Mater. 2022, 5, 4085.
- [35] J. Li, H. Cao, X. Wang, H. Zhu, Z. Dong, L. Yang, S. Yin, ACS Appl. Energy Mater. 2019, 2, 2506.
- [36] M. Vásquez-Montoya, J. F. Montoya, D. Ramirez, F. Jaramillo, J. Energy Chem. 2021, 57, 386.
- [37] H. B. Lee, N. Kumar, S. Cho, S. Hong, H. H. Lee, H. J. Kim, J. S. Lee, J. W. Kang, Adv. Energy Sustain. Res. 2023, 4, 2200128.
- [38] H. B. Lee, N. Kumar, M. M. Ovhal, Y. J. Kim, Y. M. Song, J. W. Kang, Adv. Funct. Mater. 2020, 30, 1.
- [39] H. B. Lee, N. Kumar, B. Tyagi, K. J. Ko, J. W. Kang, Sol. RRL. 2021, 5, 2000589
- [40] H. B. Lee, A. Mohamed, N. Kumar, N. H. Zain Karimy, V. V. Satale, B. Tyagi, D. H. Kim, J. W. Kang, Small Methods. 2024, 9, 2400850.
- [41] P. Shi, J. Xu, I. Yavuz, T. Huang, S. Tan, K. Zhao, X. Zhang, Y. Tian, S. Wang, W. Fan, Y. Li, D. Jin, X. Yu, C. Wang, X. Gao, Z. Chen, E. Shi, X. Chen, D. Yang, J. Xue, Y. Yang, R. Wang, Nat. Commun. 2024, 15, 2370
- [42] T. Okoroafor, A. Maalouf, S. Oez, V. Babu, B. Wilk, S. Resalati, J. Clean. Prod. 2022, 373, 133665.
- [43] D. N. Lee, Y. S. Jeon, S. C. Cho, S. U. Lee, N. G. Park, ACS Energy Lett. 2024, 9, 4172.
- [44] S. H. Lee, S. Jeong, S. Seo, H. Shin, C. Ma, N. G. Park, ACS Energy Lett. 2021, 6, 1612.
- [45] K. W. Yeom, D. K. Lee, N. G. Park, Adv. Energy Mater. 2022, 12, 2200275.
- [46] L. Yuan, Z. Wang, R. Duan, P. Huang, K. Zhang, Q. Chen, N. K. Allam, Y. Zhou, B. Song, Y. Li, J. Mater. Chem. A. 2018, 6, 19696
- [47] B. Abdollahi Nejand, I. M. Hossain, M. Jakoby, S. Moghadamzadeh, T. Abzieher, S. Gharibzadeh, J. A. Schwenzer, P. Nazari, F. Schackmar, D. Hauschild, L. Weinhardt, U. Lemmer, B. S. Richards, I. A. Howard, U. W. Paetzold, Adv. Energy Mater. 2020, 10, 1902583.
- [48] T. Abzieher, S. Moghadamzadeh, F. Schackmar, H. Eggers, F. Sutterlüti, A. Farooq, D. Kojda, K. Habicht, R. Schmager, A. Mertens, R. Azmi, L. Klohr, J. A. Schwenzer, M. Hetterich, U. Lemmer, B. S. Richards, M. Powalla, U. W. Paetzold, Adv. Energy Mater. 2019, 9, 1802995.
- [49] Q. Guo, H. Liu, Z. Shi, F. Wang, E. Zhou, X. Bian, B. Zhang, A. Alsaedi, T. Hayat, Z. Tan, *Nanoscale*. 2018, 10, 3245.
- [50] L. V. Mercaldo, E. Bobeico, A. De Maria, M. Della Noce, M. Ferrara, L. Lancellotti, A. Romano, G. V. Sannino, G. Nasti, A. Abate, P. Delli Veneri, Energy Technol. 2022, 10, 2200748.
- [51] D. Ou, W. Ye, M. H. Shang, J. Tu, J. Zheng, L. Wang, W. Yang, Z. Du, Z. Yang, ACS Appl. Mater. Interfaces. 2023, 15, 42697.